Aerosol Science and Technology

ISSN: 0278-6826 (Print) 1521-7388 (Online) Journal homepage: http://www.tandfonline.com/loi/uast20

# Induction Charging and Electrostatic Classification of Micrometer-Size Particles for Investigating the Electrobiological Properties of Airborne Microorganisms

Gediminas Mainelis , Klaus Willeke , Paul Baron , Sergey A. Grinshpun & Tiina Reponen

**To cite this article:** Gediminas Mainelis , Klaus Willeke , Paul Baron , Sergey A. Grinshpun & Tiina Reponen (2002) Induction Charging and Electrostatic Classification of Micrometer-Size Particles for Investigating the Electrobiological Properties of Airborne Microorganisms, Aerosol Science and Technology, 36:4, 479-491, DOI: 10.1080/027868202753571304

**To link to this article:** http://dx.doi.org/10.1080/027868202753571304

Published online: 30 Nov 2010.

Aerosol Science and Technology 36: 479–491 (2002)

Published by Taylor and Francis
0278-6826/02/$12.00 + .00

# Induction Charging and Electrostatic Classification of Micrometer-Size Particles for Investigating the Electrobiological Properties of Airborne Microorganisms

**Gediminas Mainelis,[1] Klaus Willeke,[1] Paul Baron,[2] Sergey A. Grinshpun,[1] and Tiina Reponen[1]**

[1]*Aerosol Research and Exposure Assessment Laboratory, Department of Environmental Health, University of Cincinnati, Cincinnati, Ohio*
[2]*CDC-NIOSH, Cincinnati, Ohio*

**Our earlier studies have shown that the electrostatic collection technique, a potentially "gentle" bioaerosol collection method, allows for efficient collection of airborne bacteria, but sensitive bacteria such as *Pseudomonas fluorescens* (*P. fluorescens*) lose their culturability during collection. We hypothesized that excessive stress was imposed on the sensitive bacteria by the sampler's conventional corona charging mechanism. In this research, we developed and built an experimental setup that allows us to analyze electrobiological properties of airborne microorganisms. In this experimental system, we imparted electric charges on airborne biological and nonbiological particles by aerosolizing them in the presence of an electric field. The charged *P. fluorescens* test bacteria and NaCl test particles were then channeled into a parallel plate mobility analyzer, which we have designed so that bacteria and inert particles carrying specific charge ranges can be extracted and made available for further analysis. When testing the experimental system, we related the extracted particle concentrations to the total particle concentration and obtained the charge distributions of these particles at different charging conditions. Our results have shown that even without charging, aerosolized *P. fluorescens* bacteria have a net negative charge and can carry up to 13,000 elementary charges per bacterium. In contrast, the NaCl particles were found to carry very few electric charges. We concluded that the electric charge carried by a bacterium consists of 2 components: its own natural charge, which can be high, and the charge imposed on it by the dispersion process. Our experiments have shown that the charge distributions on biological and nonbiological particles can be effectively manipulated by varying the external electric field during their aerosolization. Since airborne microorganisms may carry high internal electric charges, their collection by electrical field forces may be possible without first electrically charging them.**

Received 12 October 2000; accepted 8 May 2001.

This study was supported through NIOSH grant R01 OH03463. The authors are thankful for this support. G. Mainelis was partially supported by a University of Cincinnati graduate scholarship.

Address correspondence to Gediminas Mainelis. Current address and affiliation: Department of Environmental Sciences, Rutgers, The State University of New Jersey, 14 College Farm Road, New Brunswick, NJ 08902. E-mail: mainelis@envsci.rutgers.edu

## INTRODUCTION

Exposure to airborne microorganisms is usually monitored by using air samplers that have been designed for collecting airborne biological particles. Commonly used sampling methods, such as impaction and impingement, are known to affect the viability of sensitive microorganisms (Stewart et al. 1995). In the search for a "gentle" microorganism collection method, we used a modified electrostatic precipitator to collect airborne bacteria (Mainelis et al. 1999). We concluded that hardy microorganisms, such as *Bacillus subtilis* var *niger*, can be efficiently collected by electrostatic precipitation. However, sensitive bacterial cells, such as *Pseudomonas fluorescens* (*P. fluorescens*), may be inactivated by the corona discharge, which is the charging mechanism in conventional electrostatic precipitators. The corona discharge produces ozone, which is a powerful oxidant (Boelter and Davidson 1997) and may harm sensitive bacteria (Cox and Wathes 1995). Thus to explore the full potential of electrostatic precipitation as a collection method for viable bioaerosol particles, techniques other than the traditional corona discharge have to be found to impose electric charges onto the particles.

One alternative to conventional corona charging is electric charging by induction, which is achieved by generating droplets from bulk liquid in the presence of an externally applied electric field. This technique does not produce gaseous ions (Reischl et al. 1977) and has successfully been used to charge nonbiological particles. Reischl et al. (1977) modified a vibrating orifice aerosol generator by imposing an electric field

between the metal orifice, through which the liquid is dispersed, and an external metal ring. With this setup, the authors produced monodisperse particles of NaCl and were able to induce more than 10,000 elementary charges per particle. Periasamy et al. (1991) used a similar setup to generate charged dioctyl phtalate particles in a vacuum. Induction charging has also been successfully used to impart electric charges on particles aerosolized by the impulse jet technique (Choi and Delcorio 1990) and the sonic spray technique (Hirabayashi and de la Mora 1998). Erin and Hendricks (1968) applied a perturbation to a liquid jet and charged the droplets as they formed while exposed to an external electric field. With this method they produced charged uniform particles of sodium nitrate ranging from 90 to 150 $\mu$m in diameter. All these dispersion techniques were designed to produce monodisperse nonbiological particles of sizes mostly larger than those of airborne microorganisms.

Studies on water-borne microorganisms have indicated that microorganisms in a liquid may carry thousands of elementary charge units (Sherbet and Lakshmi 1973). Thus one may expect that microorganisms in the airborne state will also carry electric charges, in which case their collection by electrostatic forces would be possible without the need for prior charging. However, we are not aware of any published data on the electric charges carried by airborne microorganisms.

In this study, we have developed tools for manipulating and measuring the electric charges on airborne biological and nonbiological particles. For this purpose, we have designed and built a bioaerosol generator in which the organisms are charged by induction during their pneumatic nebulization in a modified Collison nebulizer. Collison nebulizers are widely used to aerosolize microorganisms (Chen et al. 1994; Jensen et al. 1992). We chose not to use a vibrating orifice generator to disperse biological particles because the small orifice in this kind of disperser can easily become blocked by clumped microorganisms (Jensen et al. 1994). By employing induction charging, we avoid potentially harmful ozone production that occurs during conventional corona charging. Specific features of our aerosol generation technique are discussed in detail in the following section. The charge levels on the aerosolized microorganisms, ranging from their positive to their negative charge limits, have been determined by a parallel plate mobility analyzer coupled with a particle size spectrometer. We designed the mobility analyzer to extract microorganism fractions carrying specific electric charge ranges, i.e., the mobility analyzer classifies particles according to their electrical charge. This feature was developed to be used in later studies to determine the extent to which the amount of electric charge affects the viability of airborne microorganisms. This paper is focused on the development of a bioaerosol generator with charge induction and subsequent measurements of the electric charge distributions on aerosolized micrometer-size biological and nonbiological particles.

## BIOAEROSOL GENERATOR WITH CHARGE INDUCTION

### *Apparatus*

Figure 1 is a schematic representation of the aerosol generator that we have developed and used for the dispersion and simultaneous electric charging of microorganisms. The microorganisms are dispersed through a single orifice in the center stem of a Collison nebulizer (BGI Inc., Waltham, MA). The housing of the Collison nebulizer, which acts as the impaction surface in conventional applications, is not included in this design. Passage of the nebulizer airflow, $Q_{\mathrm{NEB}}$, through the orifice creates negative pressure downstream of the sonic orifice, which pulls the liquid suspension feed into the air jet emanating from the orifice. The air jet, in turn, breaks up the liquid into polydisperse droplets, which pass through the induction ring positioned 9 mm from the Collison's orifice. The ring's inner diameter is 37 mm and its plane is oriented perpendicular to the orifice axis. Application of a positive or negative voltage, $V_{\mathrm{INDUCTION}}$, to the stainless steel Collison stem (while the induction ring is grounded) creates an electric field in the axial direction that induces electric charges onto the droplets as they are being formed from the liquid exiting the liquid feed tube in the Collison stem. As the droplets pass through the induction ring, they are surrounded by a dry, clean airflow, $Q_{\mathrm{DRY1}}$, that separates the droplets from each other and starts drying them. After the liquid content of each charged droplet containing a bacterium has evaporated, the electric charge remains on the bacterium. Since the aerosolization process produces droplets of a wide size distribution, including droplets larger than 5 $\mu$m (May 1973), the aerosol generator is slightly inclined towards the ground so that the largest droplets settle to the bottom of the aerosol generator and are drained. The drained liquid is not recirculated. Addition of more dry air, $Q_{\mathrm{DRY2}}$, completes the desiccation of the droplets that have not been drained so that only charged airborne microorganisms and much smaller droplet residues leave the aerosol generator. This technique is also applicable to nonbiological particles. To minimize particle losses in the aerosol generator due to electrostatic attraction to nonconducting surfaces, all aerosol generator parts are made of metal.

### *Charging Process*

When air is forced through the orifice of a Collison nebulizer, it breaks up the liquid feed into a dispersion of droplets of a very wide size distribution (May 1973). Due to the wide size distribution of the droplets formed and the complexity of the jet breakup, the development of a precise theory on droplet charging by induction would be very complex and beyond the scope of this paper. However, theories developed for simpler cases reveal some key insights.

Hendricks (1973) found that for a circular liquid jet issuing from a reservoir and traveling through a concentric electrode,

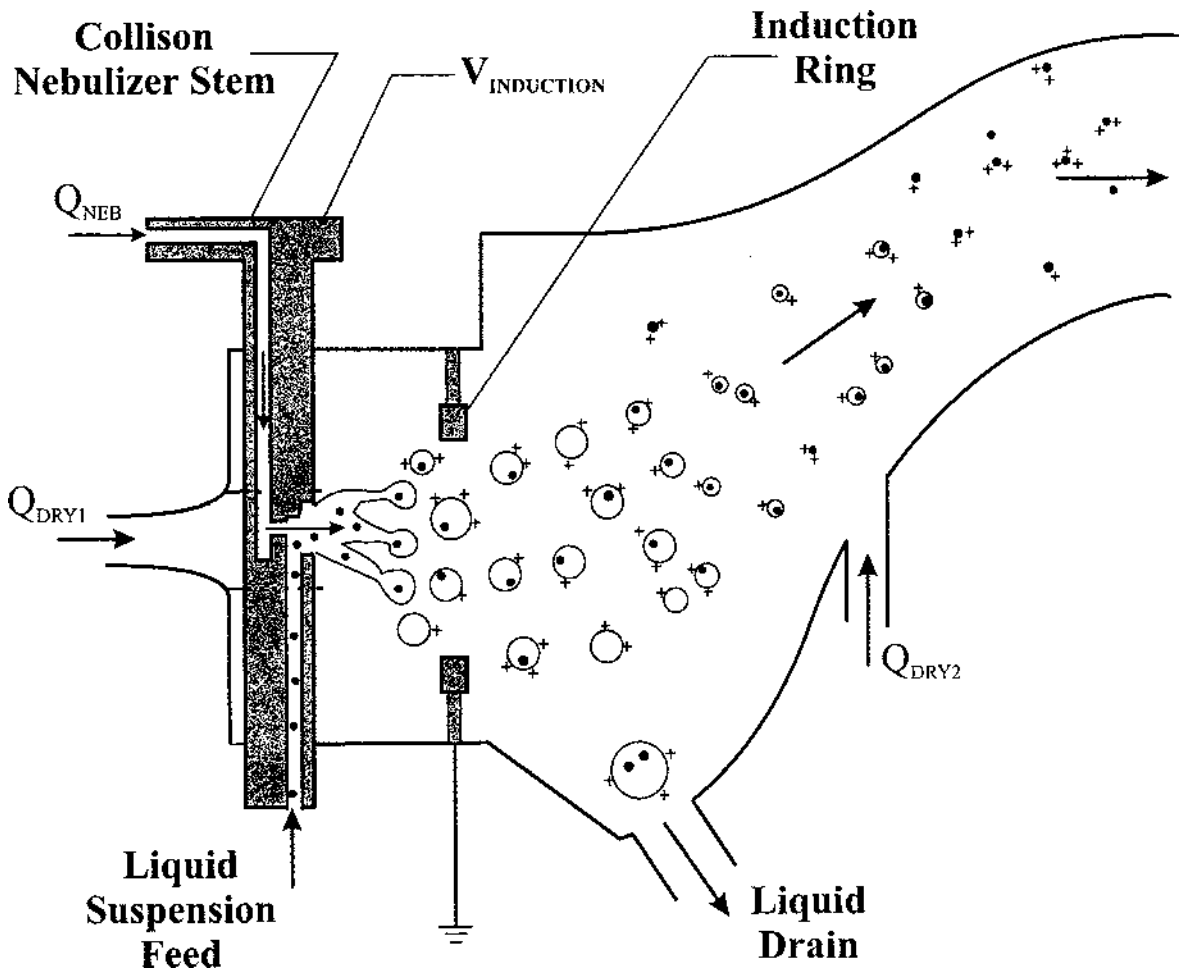


**Figure 1.** Bioaerosol generator with charge induction. Shown when a positive induction voltage is applied.

the electric charge, $q$, induced on a droplet can be calculated as

$$q = \frac{8\pi V_{\text{INDUCTION}} \varepsilon_0 r^3}{3a^3 \ln(b/a)}, \quad [1]$$

where $V_{\text{INDUCTION}}$ is the induction voltage, $\varepsilon_0$ is the gas permittivity, $r$ is the radius of the droplets formed from the jet, $a$ is the radius of the jet, and $b$ is the inner radius of the charging ring electrode. A similar expression was derived by Choi and Delcorio (1990), who concluded that when an uncharged liquid droplet enters a region in which there exists a positive electric field, the droplet becomes a dipole: a negative charge accumulates on the surface, while a region of positive charge develops in the inner portion of the droplet. In a negative electric field, the particle's surface becomes positively charged and the particle's interior becomes negatively charged. This is due to the migration of electrons to the surface of the droplet. Atten and Oliveri (1992) examined the kinetics of droplet charging when a step voltage is applied to the external cylindrical electrode just after a droplet has detached from the jet. In this case, according to the authors, the charging occurs continuously through distributed resistance and capacitance.

Reischl et al. (1977) found that for dispersion through a flat orifice the amount of induced charge can be described as

$$q = \frac{4\pi \varepsilon_0 r l \alpha V_{\text{INDUCTION}}}{eh}, \quad [2]$$

where $l$ is the distance between orifice and droplet at the instant of droplet separation, $h$ is the distance between induction electrode and orifice, $e$ is the elementary charge, and $\alpha$ is a correction factor for the nonuniformity of the electric field. Since the droplet production from a Collison's orifice can be considered to be from a flat orifice, Equation (2) is applicable to our aerosol generator. However, only limited information is available on the distance between orifice and droplet at the instant of droplet separation, which in turn limits the use of Equation (2). We note, however, that the amount of induced charge is directly proportional to the induction voltage and the droplet radius.

## ELECTRIC MOBILITY ANALYZER

### *Apparatus*

To measure the polarity and magnitude of electric charges on micrometer-size biological and nonbiological airborne particles, we designed and built an electrical mobility analyzer and coupled it with an optical particle counter. By extracting particles of specific electrical mobility and measuring their sizes, we determined the number of elementary electrical charges carried by these particles. Figure 2a shows the top view of this device, and its side view is depicted in Figure 2b. The analyzer has parallel plate geometry and consists of 3 main sections:

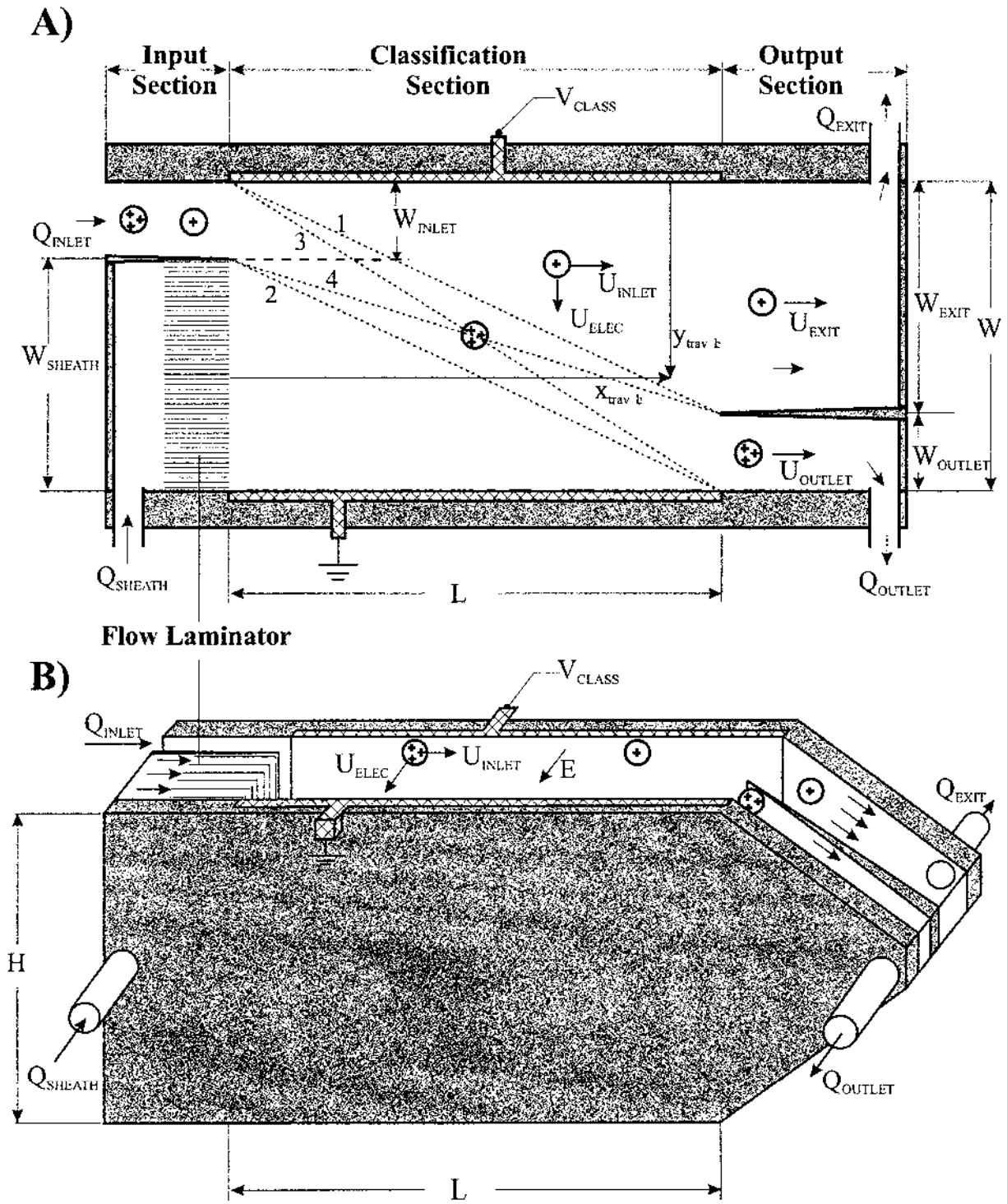


**Figure 2.** Parallel plate mobility analyzer: (a) top view; (b) side view.

the input section (shown on the left in Figure 2), where the charged particles enter the classifier through the inlet channel (top left in Figure 2a) in parallel to sheath air; the classification section (middle part in Figure 2), where the particles are subjected to an electric field; and the output section (shown on the right in Figure 2), where the particles of interest are extracted through the outlet channel (bottom right in Figure 2a) and the rest of the particles leave through the exit channel. The lengths of these sections are 7.5, 30.5, and 15.0 cm, respectively. The width of the analyzer's outlet channel, $W_{\mathrm{OUTLET}} = 3$ mm, is equal to that of the inlet channel, $W_{\mathrm{INLET}}$; the width of the analyzer's exit channel, $W_{\mathrm{EXIT}} = 9$ mm, is equal to that of the sheath air channel, $W_{\mathrm{SHEATH}}$. The analyzer's height, $H$, and total width, $W$, are 10.1 and 1.2 cm, respectively. Two stainless steel plates imbedded in insulating material form the analyzer's main body. One of the analyzer's plates (the lower plate in Figure 2a) was always grounded, while the other plate (upper plate in Figure 2a) was connected either to a positive or a negative voltage, $V_{\mathrm{CLASS}}$, depending on the polarity of the particles being analyzed. The classifier was used with the plates upright (as shown in Figure 2b) so that the electric field acted at right angle to gravity.

### *Operation of the Analyzer*

To ensure laminar airflow throughout the analyzer, the airflow rates in the inlet and outlet channels were kept at the same ratios as the widths of the respective channels:

$$\frac{Q_{\mathrm{INLET}}}{Q_{\mathrm{SHEATH}}} = \frac{W_{\mathrm{INLET}}}{W_{\mathrm{SHEATH}}} = \frac{1}{3}, \qquad [3]$$

$$\frac{Q_{\mathrm{OUTLET}}}{Q_{\mathrm{EXIT}}} = \frac{W_{\mathrm{OUTLET}}}{W_{\mathrm{EXIT}}} = \frac{1}{3}, \qquad [4]$$

where $Q_{\mathrm{INLET}}$, $Q_{\mathrm{SHEATH}}$, $Q_{\mathrm{OUTLET}}$, and $Q_{\mathrm{EXIT}}$ represent the airflows through the inlet, sheath, outlet, and exit channels, respectively (as shown in Figure 2). Assuming laminar airflow, and equality between air and particle velocity, the velocity of a particle entering the classification section and moving in the $x$ direction, $U_{\mathrm{INLET}}$, is equal to the sheath air velocity, $U_{\mathrm{SHEATH}}$:

$$U_{\mathrm{INLET}} = \frac{Q_{\mathrm{INLET}}}{W_{\mathrm{INLET}} H} = U_{\mathrm{SHEATH}} = \frac{Q_{\mathrm{SHEATH}}}{W_{\mathrm{SHEATH}} H}, \qquad [5]$$

where $H$ is the height of the classifier. Since the airflows $Q_{\mathrm{INLET}}$ and $Q_{\mathrm{SHEATH}}$ are kept at the same ratio as the widths of their respective entrance channels (as shown in Equations (3) and (4)), the particle velocity in the $x$ direction can also be expressed as

$$U_{\mathrm{INLET}} = \frac{Q_{\mathrm{INLET}} + Q_{\mathrm{SHEATH}}}{(W_{\mathrm{INLET}} + W_{\mathrm{SHEATH}})H} = \frac{Q}{WH}, \qquad [6]$$

where $Q$ is the total airflow entering and leaving the analyzer. When a voltage, $V_{\mathrm{CLASS}}$, is applied across the plates, charged particles are deflected from their original paths due to the action of electrostatic force $F_{\mathrm{elec}}$:

$$F_{\mathrm{elec}} = ne\frac{V_{\mathrm{CLASS}}}{W}. \qquad [7]$$

When the drag force on a particle becomes equal to the applied electrostatic force, the particle moves with terminal velocity $U_{\mathrm{ELEC}}$:

$$U_{\mathrm{ELEC}} = \frac{neC_c}{3\pi\eta d_p}\frac{V_{\mathrm{CLASS}}}{W} = Z_p\frac{V_{\mathrm{CLASS}}}{W}, \qquad [8]$$

where

$$Z_p = \frac{neC_c}{3\pi\eta d_p} \qquad [9]$$

and $C_c$ is the slip correction factor, $\eta$ is the dynamic viscosity of air, $d_p$ is the particle diameter, and $Z_p$ represents the electrical mobility of the particle. Thus particle motion inside the classifier in the $x$ direction is described by velocity vector $U_{\mathrm{INLET}}$, while its motion in the $y$ direction (direction of the applied electric field $E$) is described by $U_{\mathrm{ELEC}}$.

When a particle with mobility $Z_p$ enters the analyzer, it needs time, $t$, to reach the outlet of the analyzer. During that time, the particle travels distance $y_{\mathrm{travel}}$ in the $y$ direction and distance $x_{\mathrm{travel}}$ in the $x$ direction, as shown in Figure 2a. Thus

$$t = \frac{y_{\mathrm{travel}}}{U_{\mathrm{ELEC}}} = \frac{y_{\mathrm{travel}} W}{Z_p V_{\mathrm{CLASS}}} = \frac{x_{\mathrm{travel}}}{U_{\mathrm{INLET}}} = \frac{x_{\mathrm{travel}} WH}{Q}. \qquad [10]$$

The mobility of a particle reaching the analyzer's outlet can also be expressed as

$$Z_p = \frac{y_{\mathrm{travel}} Q}{x_{\mathrm{travel}} H}\frac{1}{V_{\mathrm{CLASS}}}. \qquad [11]$$

For each particle reaching the analyzer's outlet, $x_{\mathrm{travel}}$ is the same, $L$. However, the $y_{\mathrm{travel}}$ of each particle may vary from $\frac{1}{2}W$ to $W$ depending on its mobility and the position in the analyzer's inlet. Thus penetration of particles through the electrical mobility analyzer is usually described by its transfer function, $\Omega$, which indicates the probability that a particle having an electrical mobility $Z_p$ will be observed at the analyzer's outlet. The transfer function depends on the electrical mobility, analyzer's geometry, and applied voltage, i.e., $\Omega = \Omega\,(V_{\mathrm{CLASS}}, Z_p)$. Since the width of the inlet channel, $W_{\mathrm{INLET}}$, is equal to that of the outlet channel, $W_{\mathrm{OUTLET}}$, the analyzer's transfer function will have the shape of an isosceles triangle and there will be one critical mobility, $Z_{p,\mathrm{crit}}$ at which all of the aerosol particles introduced into the classifier are extracted (Brown 1997), i.e., $\Omega\,(V_{\mathrm{CLASS}}, Z_{p,\mathrm{crit}}) = 1$. In this case, the distance traveled by particles of mobility $Z_{p,\mathrm{crit}}$ is $y_{\mathrm{travel}} = \frac{3}{4}W$; their extreme trajectories are numbered 1 and 2 in Figure 2a and

$$Z_{p,\mathrm{crit}} = \frac{3QW}{4LHV_{\mathrm{CLASS}}}. \qquad [12]$$

For electrical mobilities that differ only incrementally from this critical value, less of the aerosol will be extracted, i.e., $\Omega < 1$. Particles of highest and lowest mobility that will still be extracted from the analyzer have trajectories 3 and 4, respectively.

For particles with trajectories 4, $y_{\text{travel}} = \frac{1}{2}W$ and their mobilities can be described as $Z_p = \frac{2}{3}Z_{p,\text{crit}}$; for particles with trajectories 3, $y_{\text{travel}} = W$ and their mobilities can be described as $Z_p = \frac{4}{3}Z_{p,\text{crit}}$. Since these points represent the basis of the transfer function's triangle, the whole transfer function can be derived as

$$\begin{aligned}
&\Omega = 0 \quad \text{for} Z_p > \frac{4}{3}Z_{p,\text{crit}} \quad \text{and} \quad Z_p < \frac{2}{3}Z_{p,\text{crit}};\\
&\Omega = 4\left(1 - \frac{V_{\text{CLASS}}LH}{WQ}Z_p\right) \quad \text{for } \frac{4}{3}Z_{p,\text{crit}} \geq Z_p \geq Z_{p,\text{crit}};\\
&\Omega = 1 \quad \text{for } Z_p = Z_{p,\text{crit}} = \frac{3QW}{4LHV_{\text{CLASS}}};\\
&\Omega = 4\left(\frac{V_{\text{CLASS}}LH}{WQ}Z_p - \frac{1}{2}\right) \quad \text{for } \frac{2}{3}Z_{p,\text{crit}} \leq Z_p \leq Z_{p,\text{crit}}.
\end{aligned} \tag{13}$$

Thus particles measured downstream of the analyzer have electrical mobilities varying from $Z_p = \frac{2}{3}Z_{p,\text{crit}}$ to $Z_p = \frac{4}{3}Z_{p,\text{crit}}$ with their median mobility equal to $Z_{p,\text{crit}}$, which corresponds to the peak of the transfer function.

The number of particles measured downstream of the analyzer when certain $V_{\text{CLASS}}$ is applied depends not on transfer function alone but rather on its product with the particle mobility distribution upstream of the analyzer, $N = N(Z_p)\ \Omega\ (V_{\text{CLASS}}, Z_p)$. Thus depending on the $N(Z_p)$, the mobility distribution of particles downstream of the analyzer, may no longer have the shape of an isosceles triangle. In that case, the median particle mobility will also be different from $Z_{p,\text{crit}}$. Our calculations have shown that for the current geometry of the mobility analyzer and for wide and slowly changing mobility distribution functions, such as $N(\sim 1/Z_p)$ or $N(\sim 1/Z_p^2)$, the shift in median mobility is <5%; for lognormal distribution of $N(Z_p)$, the shift in median mobility is about 6%. The determined shift in median mobility is small and does not exceed experimental error. Thus presuming that mobility distributions of aerosolized particles are slowly changing functions, with about 5% error we can assume that median mobility of extracted particles is equal to $Z_{p,\text{crit}}$. This assumption simplifies our calculations and, by combining Equations (9) and (12), we can express the median number of elementary charges, $n_{\text{crit}}$, carried by extracted particles as

$$n_{\text{crit}} = n(Z_{p,\text{crit}}) = \frac{3}{4}W\frac{Q}{LHV_{\text{CLASS}}}\frac{3\pi\eta d_p}{eC_c}. \tag{14}$$

As particles in the outlet are measured with an optical particle counter in narrow particle diameter ranges, we can calculate the median number of elementary charges carried by these particles when a certain voltage $V_{\text{CLASS}}$ is applied across the plates of the classifier.

## MEASUREMENT METHODS

### *Experimental Setup*

The primary purpose of this study was to design and build an experimental facility for investigating the electrobiological properties of airborne microorganisms. This facility is schematically shown in Figure 3. In our setup, biological and nonbiological particles are charged by means of induction charging and their charges are then measured by the electrical mobility analyzer coupled with an optical particle counter (OPC, model 1.108, Grimm Technologies Inc., Douglasville, GA). This experimental arrangement allows us to determine the physical characteristics of tested aerosol particles. A microbial sampler, as shown in Figure 3, is added as a tool for microbiological characterization of viable airborne microorganisms.

While aerosolized from a liquid suspension through a Collison nebulizer's stem at a flow rate, $Q_{\text{NEB}}$, of 1.2 L/min, the particles were charged as described in the previous section. The air entering the nebulizer was dry, filtered, and under a positive pressure of 20 psi ($1.4 \cdot 10^5$ Pa). Four different levels of charging were achieved by applying charging voltages, $V_{\text{INDUCTION}}$, of 0, −100, −3,000, and +3,000 V between the grounded induction ring and the Collison's stem. The charging voltage was applied through an external power source (DC Power Supply HP 6516A, Hewlett Packard Inc., Rockaway, NJ). Separation and initial drying of the dispersed droplets was achieved by the airflow $Q_{\text{DRY1}}$ at 50 L/min, and the final drying was achieved through airflow $Q_{\text{DRY2}}$ at 30 L/min. Both airflows were dry and HEPA filtered. The largest droplets gravitationally settled to the aerosol generator's bottom and were drained off. The total airflow, $Q_{\text{TOTAL}}$, of 80 L/min entered an open and horizontally oriented sampling chamber from which the aerosol particles were sampled into the electrical mobility analyzer at a flow rate $Q_{\text{INLET}}$ of 6.7 L/min. The analyzer's outlet flow rate, $Q_{\text{OUTLET}}$, was also 6.7 L/min, and the sheath airflow, $Q_{\text{SHEATH}}$, as well as the exit airflow, $Q_{\text{EXIT}}$, were set at 20.1 L/min (see also Equations (3) and (4)). Two stable external power sources (DC Power Supply HP 6516A, Hewlett Packard Inc., Rockaway, NJ and DC Power Supply RHR, Spelman Inc., Bronx, NY) supplied the analyzer's classification voltage, $V_{\text{CLASS}}$, between 0 and ±4,500 V. The concentrations and size distributions of the particles entering the analyzer, $C_{\text{INLET}}$, and of the classified particles leaving the analyzer, $C_{\text{OUTLET}}$, were determined using 2 identical OPCs (model 1.108, Grimm Technologies Inc., Douglasville, GA), shown as OPC1 and OPC2 in Figure 3. In some experiments, we also measured the concentration and size distribution of particles exiting the analyzer, $C_{\text{EXIT}}$. This was done by using a third OPC (model 1.108, Grimm Technologies Inc). This counter is not shown in Figure 3, but later in the text it is referred to as OPC3. Each Grimm particle counter was operated at a flow rate, $Q_{\text{OPC}}$, of 1.2 L/min and measured particle concentrations in 16 size channels, ranging from 0.3 $\mu$m to 20 $\mu$m. Since we were concerned with particles of bacterial size, only the first 8 channels measuring particles from 0.3 $\mu$m to 3 $\mu$m

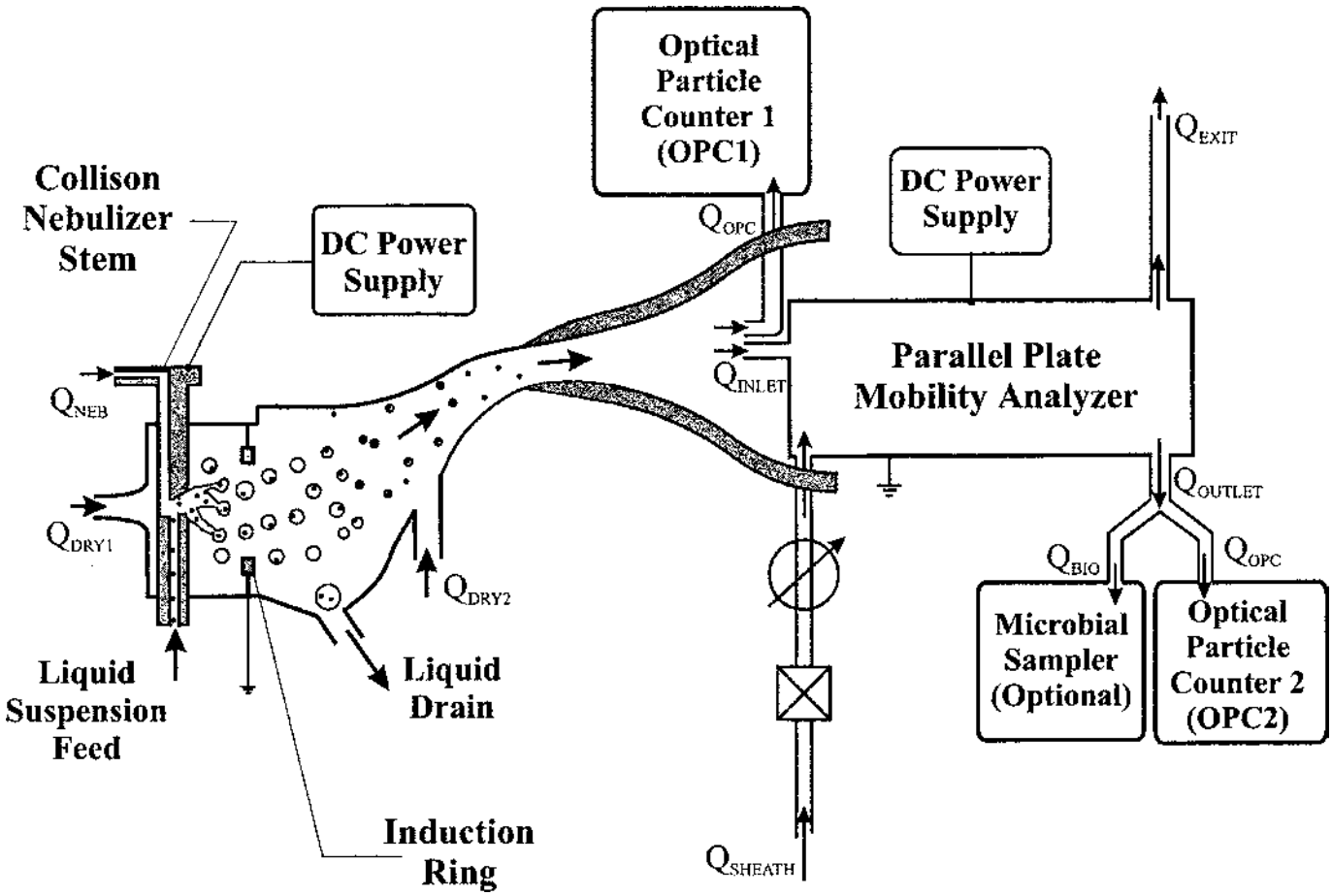


**Figure 3.** Experimental setup.

were used. Also, to avoid the effect of coincidence, concentration of airborne particles was kept well below the counting limit of the OPCs. For studies on the viability of extracted, charged microorganisms we can add a microbial sampler to the outlet flow.

To minimize losses of charged particles in the system, all sampling lines beyond the charging point were made of metal and all devices measuring and collecting charged particles were positioned as close as possible to the particle source. All airflow rates in the system were monitored with flow meters calibrated with a Buck calibrator (A.P. Buck, Inc., Orlando, FL). The entire test system was placed in a Class II, Type B2, biological safety cabinet (SterilchemGARD; Baker Company, Sanford, ME) so that the uncollected aerosol particles were properly removed. The temperature was kept at 22–26°C and the relative humidity of the drying and sheath flows at 30–50% during all experiments. These parameters were monitored by sensors (models TRH-100-20FT and P300-5PSID, Pace Scientific, Inc., Charlotte, NC) and recorded by a "Pocket Logger" (model XR440, Pace Scientific) connected to a personal computer.

### *Experimental Procedures*

At the start of each experiment, the system was operated without aerosolizing particles until 0 particle background was achieved, as measured with the OPCs. In the next step, particle aerosolization was activated and the OPC2 readings were checked to ensure that no particles passed through the classifier's outlet when no classification voltage was applied. Then a preselected charging voltage, $V_{INDUCTION}$, was applied and the OPC1 readings were checked for aerosol concentration stability. Before starting the measurements of particle electrical charge, we measured the concentration and size distribution of particles exiting the analyzer, $C_{EXIT}$. Those measurements were performed using the OPC3 and its readings were compared with those of OPC1. If both particle counters were reading the same numbers, i.e., there were no significant particle losses inside the analyzer, then the classifier's voltage, $V_{CLASS}$, was increased in a step-wise manner from 0 V to −4,500 V for measuring particles carrying a net negative charge and from 0 V to +4,500 V for measuring particles carrying a net positive charge.

For each $V_{CLASS}$ value, particle concentrations $C_{INLET}$ and $C_{OUTLET}$ were simultaneously measured with OPC1 and OPC2

for 30 s. Since both OPCs measure particles in 16 size channels, a polydisperse aerosol can be analyzed by assuming a monodisperse aerosol fraction in each size channel. Thus each aerosol fraction measured in an OPC2 size channel had a specific median electrical mobility corresponding to the applied classification voltage $V_{CLASS}$ and the average particle diameter of that size channel. The median number of elementary charges, $n$, carried by these particles can then be calculated through Equation (14), where $d_p$ is the average particle diameter of that channel. By comparing $C_{INLET}$ and $C_{OUTLET}$ for the same size channel we determined the fraction, $F_n$, of particles with average diameter $d_p$ carrying median number $n$ of elementary charges at a given $V_{CLASS}$:

$$F_n(d_p, V_{CLASS}) = \frac{C_{OUTLET}(d_p, V_{CLASS})}{C_{INLET}(V_{CLASS})}. \qquad [15]$$

By performing the same calculation for all $V_{CLASS}$ values we determined the overall charge distribution for particles of diameter $d_p$ at a specific charging condition. These measurements were performed for each charging condition and for each kind of test particle. The overall charge distribution for each experimental condition was determined 3 times. The average value and standard deviation of those measurements are presented in the Results section.

### *Test Particles*

In this study we tested NaCl particles (representatives of nonbiological particles) and vegetative cells of *P. fluorescens* (representatives of biological particles). The rod-shaped Gram-negative *P. fluorescens* bacteria are commonly found in ambient air (Nevalainen 1989; Górny and Dutkiewitz 1998) and represent sensitive bacteria (Neidhardt et al. 1990). These vegetative cells range from 0.7 to 0.8 $\mu$m in diameter and 1.5 to 3 $\mu$m in length (Palleroni 1984). Stock cultures of *P. fluorescens* (ATCC 13525) were obtained from the American Type Culture Collection (Rockville, MD). For each experiment a fresh *P. fluorescens* culture was grown in trypticase soy broth (Becton Dickinson Microbiology Systems, Cockeysville, MD) at 30°C for 18 h in a gyrotory water bath shaker (Model G76, New Brunswick Scientific Co., Edison, NJ). The *P. fluorescens* cells were harvested from their suspensions by centrifugation at 5050 g for 7 min (Sorval RC-5B, Sorval Co., Newton, CT). The resulting pellets were washed 3 times with deionized and sterilized water (5 Stage Milli-Q Plus System, Millipore Corp., Bedford, MA). To obtain suspensions of desired bacterial density, the initial washed suspension of the microorganism was diluted with deionized and sterilized water. The resulting concentrations of bacteria in the air ranged from 400 to 800 cells/cm$^3$.

In the nonbiological particle category, NaCl was chosen because it is frequently used in testing filters (Huang et al. 1996; Qian et al. 1997; Heikkinen 2000). Charging experiments have also been performed using NaCl particles (Reischl et al. 1977). They were produced by aerosolizing 0.1% w/w NaCl solution, prepared by dissolving 1 g of reagent quality NaCl (FisherChemical Co., Fair Lawn, NJ) into 1 L of deionized and sterilized water (5 Stage Milli-Q Plus System).

## EXPERIMENTAL RESULTS AND DISCUSSION

First, by comparing the readings of OPC1 and OPC3 using procedures described above, we determined the extent of particle losses inside the analyzer. This comparison showed that the concentration of particles entering the analyzer is very similar to that exiting the analyzer, i.e., there are virtually no particle losses. This result was true for all 3 charging conditions.

In our first set of experiments we determined the optical particle size distributions of *P. fluorescens* bacteria entering and leaving the mobility analyzer when an induction voltage of −3,000 V was applied during their dispersion. The results presented in Figure 4 show that the optical particle size distribution of bacteria entering the classifier, $C_{INLET}$, has a peak between 0.5 and 0.65 $\mu$m and that the majority of bacteria, almost 95%, are counted in the 3 channels between 0.5 $\mu$m and 1 $\mu$m. The particles measured between 0.3 $\mu$m and 0.5 $\mu$m are considered to be mostly droplet residues and bacterial fragments but not bacteria (Terzieva et al. 1996). The observed size distribution of *P. fluorescens* bacteria is similar to the one reported by Qian et al. (1995), who used an LAS-X optical particle size spectrometer (PMS Inc., Boulder, CO). The size distributions of bacteria selected by the analyzer ($C_{OUTLET}$) at different $V_{CLASS}$ values have the same particle size spectrum as the bacteria entering the classifier; i.e., they peak between 0.5 and 0.65 $\mu$m, with the majority of bacteria in the size range between 0.5 and 1 $\mu$m. This observation indicates that most of the bacteria adequately

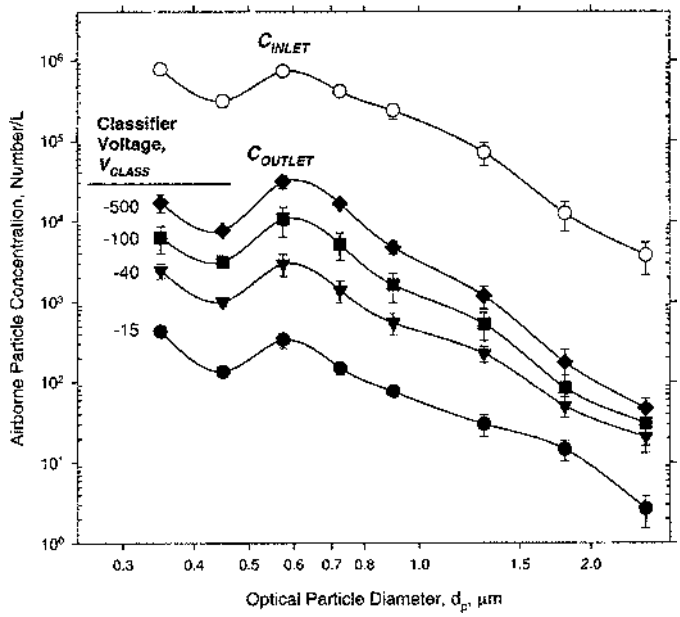


**Figure 4.** Typical particle size distributions of airborne *P. fluorescens* bacteria (induction voltage = −3,000 V).

pass through the classifier without changing the shape of their size distribution. Since about 95% of the bacteria entering and leaving the classifier are measured in the 3 channels between 0.5 and 1.0 $\mu$m, the middle channel was selected to represent the bacterial diameter. The selected channel measures particles between 0.65 and 0.8 $\mu$m and its average diameter, $d_p$, is 0.73 $\mu$m. This average optical diameter of *P. fluorescens* bacteria is similar to 0.7 $\mu$m average optical and 0.78 $\mu$m average aerodynamic diameters reported by Qian et al. (1995), who used an LAS-X optical particle size spectrometer (PMS Inc., Boulder, CO) and aerosizer aerodynamic size spectrometer (Amherst Process Instruments Inc, Hadley, MA), respectively.

Our charging experiments show that the aerosolized *P. fluorescens* bacteria have a wide bipolar charge distribution, which can be manipulated with the newly-built charging device, see Figure 5. The charge distribution was determined using Equation (15), with $d_p = 0.73$ $\mu$m. The left-hand figures show the entire charge spectrum, while the right-hand figures show the same data near the 0 charge level. For the described configuration of the experimental setup and for the chosen $d_p$, the highest number of average elementary charges measured, 16,550, corresponds to $V_{\text{CLASS}} = 5$ V and the lowest number of average elementary charges measured, 18, corresponds to $V_{\text{CLASS}} = 4{,}500$ V. This study was focused on measuring and manipulating the electric charges on airborne microorganisms for the purpose of collecting particles by electrostatic means, which requires particles charged at a relatively high level. For this reason, the configuration of the experimental setup was not modified to analyze particles carrying <18 elementary charges.

First, we determined the electric charge distribution of the aerosolized bacteria when $V_{\text{INDUCTION}} = 0$ V, i.e., when no induction voltage is applied during the dispersal of the bacteria. In this case, as seen in Figure 5, the airborne *P. fluorescens* bacteria are highly charged and carry up to 13,000 positive or negative charges and the net electric charge on these bacteria is negative. This corroborates the observation by Sherbet and Lakshmi (1973), who measured the electric charges of bacteria suspended in liquid. They found that liquid-borne bacteria generally contain electric charges in their cell wall. When we aerosolized bacteria in a slightly negative induction field ($V_{\text{INDUCTION}} = -100$ V),

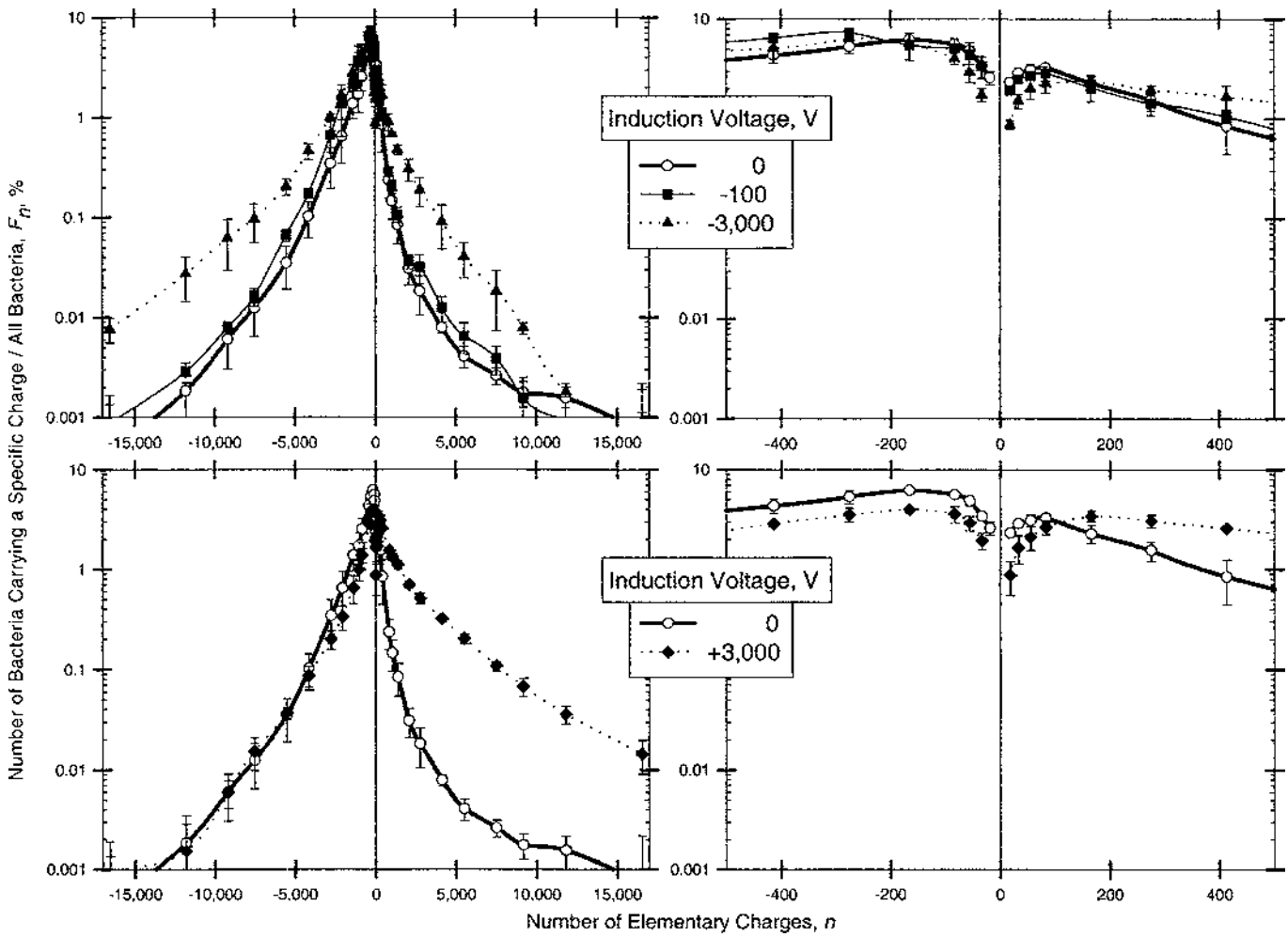


**Figure 5.** Charge distribution of *P. fluorescens* bacteria (0.65–0.8 $\mu$m) at different charging conditions.

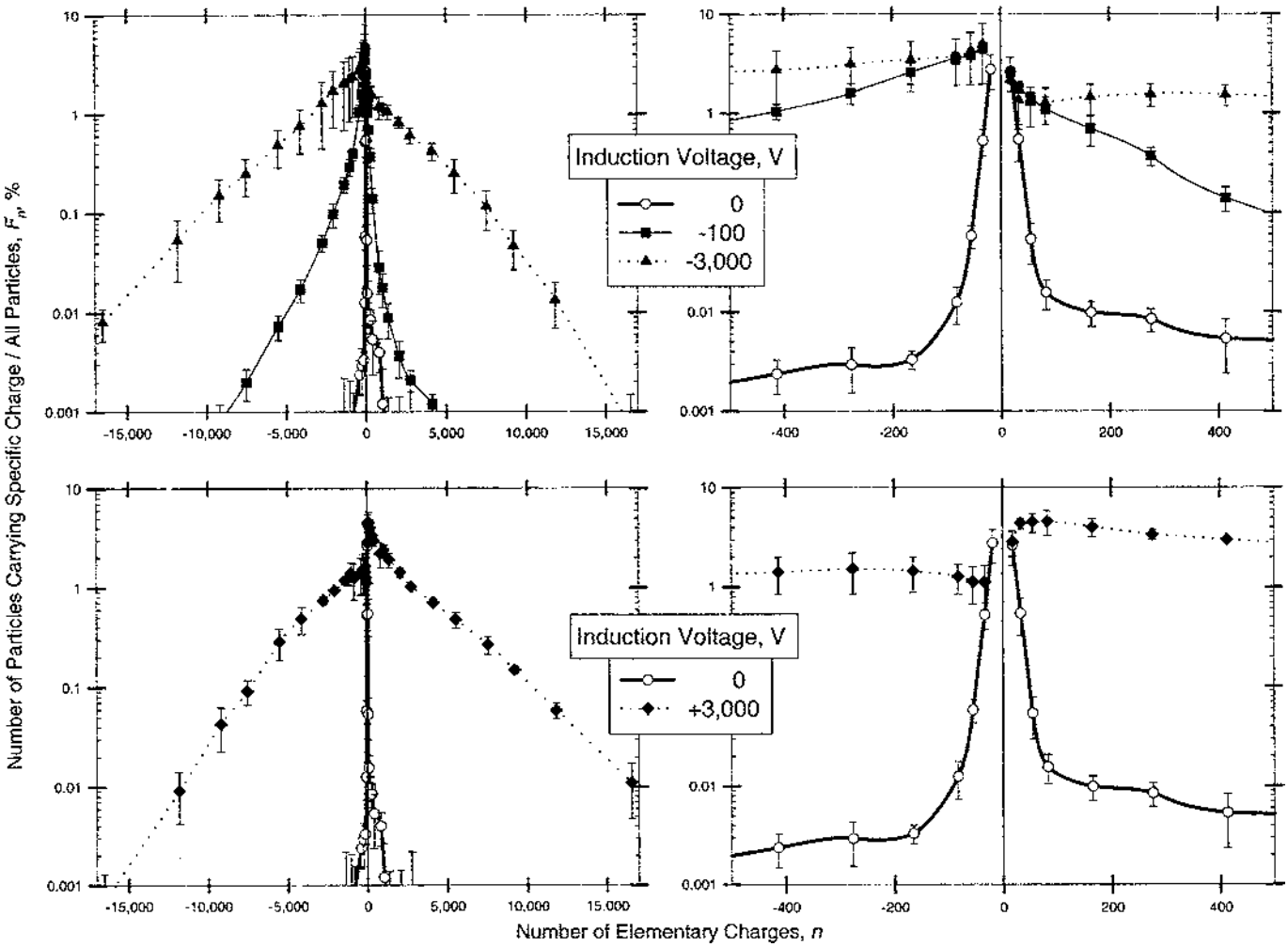


**Figure 6.** Charge distribution of NaCl particles (0.65–0.8 $\mu$m) at different charging conditions.

the electric charge distribution on the bacteria changed only slightly, see Figure 5. However, when *P. fluorescens* bacteria are dispersed in a highly negative induction field, the net charge on the bacteria becomes more negative and the number of highly negatively charged bacteria increases more than 10 times, as seen from the negative 3,000 volt curve at the top left of Figure 5. The fraction of bacteria carrying fewer than 165 elementary charges decreases by about 30%, as seen in the curves at the top right of Figure 5. When the bacteria are dispersed in a positive induction field, the net charge on the bacteria becomes positive and the number of highly positively charged bacteria increases more than 10 times, as seen from the positive 3,000 V curve at the bottom left of Figure 5. The fraction of bacteria carrying fewer than 165 elementary charges decreases by about 40% when compared to bacteria aerosolized with no induction voltage applied, as seen from the curves at the bottom right of Figure 5. To our knowledge, this is the first time that electric charge distributions have been measured on airborne microorganisms.

In our second set of experiments, we analyzed the electric charges carried by NaCl particles of the same size as the *P. fluorescens* bacteria (0.65–0.8 $\mu$m). The resulting data are shown in Figure 6, which is organized in the same way as Figure 5. As seen from Figure 6, NaCl particles, when dispersed without any induction voltage applied, carry a very low number of elementary charges. From the shape of the 0 V induction curve, we can deduce that a major portion of the NaCl particles carries $<18$ elementary charges (below the measurement limit with the current experimental setup). This conclusion agrees with the results obtained by Forsyth et al. (1998), who determined the average charge on NaCl particles dispersed with a regular Collison nebulizer (0.1% w/w NaCl solution). According to these authors, 0.7 $\mu$m NaCl particles on average carry about 10 elementary charges. A study by Johnston et al. (1985) reported 5 elementary charges on NaCl particles dispersed with a regular Collison nebulizer. Bassett (1975) observed that ultrasonic atomization of sodium nitrate solution produced 2–20 $\mu$m droplets of both polarities with a very low charge on the majority of droplets.

When we applied an induction voltage of −100 V during the dispersion of the same NaCl solution, the particle charge distribution became wider and net negative. We observed that some particles carried more than 5,000 negative charges and some more than 3,000 positive charges. After applying a high induction voltage of −3,000 V, the electric charge distribution of NaCl particles became very wide and more net negative. We measured particles carrying more than 15,000 negative elementary charges, and the fraction of particles carrying between 165 and 1,000 negative charges increased more than 1,000 times. At the same time, the fraction of positively charged particles also increased. When an induction voltage of +3,000 V was applied, the particle charge distribution became strongly net positive, with some particles carrying more than 15,000 positive charges. We think that the spread in the charge distribution is caused by the variation in the jet liquid length during droplet breakup and by the spread in droplet sizes, since both of these affect the electrical charge and mobility of a particle (Reischl et al. 1977).

The data discussed above are plotted in Figures 7 and 8 to allow a side-by-side comparison of the charge distributions of *P. fluorescens* bacteria and NaCl particles. Each chart presented in Figures 7 and 8 compares charge distributions measured at the same charging conditions. Figure 7 compares the data over the entire wide electric charge distribution range, while Figure 8 shows the same data near the 0 charge level. As seen in the uppermost chart of Figure 7, the charge distribution of *P. fluorescens* bacteria is very wide, while very low charges are measured on NaCl particles, when no induction voltage is applied. When a low induction voltage of −100 V is applied, the electric charge distribution on NaCl particles becomes wider, approaching the electric charge distribution of *P. fluorescens* bacteria. At high induction voltages of +3,000 V and −3,000 V, NaCl particles become more charged than their biological counterparts. Analyses of the number of charges in the close to 0 charge level range reveals essentially the same trend. As seen in Figure 8, a large fraction of bacteria carries electric charges even when no induction voltage is applied during their aerosolization. The fraction of NaCl particles carrying from 165 to 500 elementary charges is from 2 to 3 decades lower than that of the bacteria. When a high induction voltage is applied, the fraction of charged NaCl particles increases and both charge distributions become similar.

The striking difference between the charge distributions of *P. fluorescens* bacteria and NaCl particles can be attributed to the very different nature of these particles. When droplets are produced by a spray process, they acquire electric charges (Hendricks 1973). This results from disturbing the electrical double layers during the formation of new liquid surfaces (Johnston et al. 1985). Once a droplet containing a bacterium (or NaCl) has acquired an electric charge, that electric charge remains on the bacterium after the liquid content of the droplet has evaporated. Thus when no induction charging is applied, the charges carried by the bacteria consist of 2 components: their own natural charge, which can be high, and the charge imposed

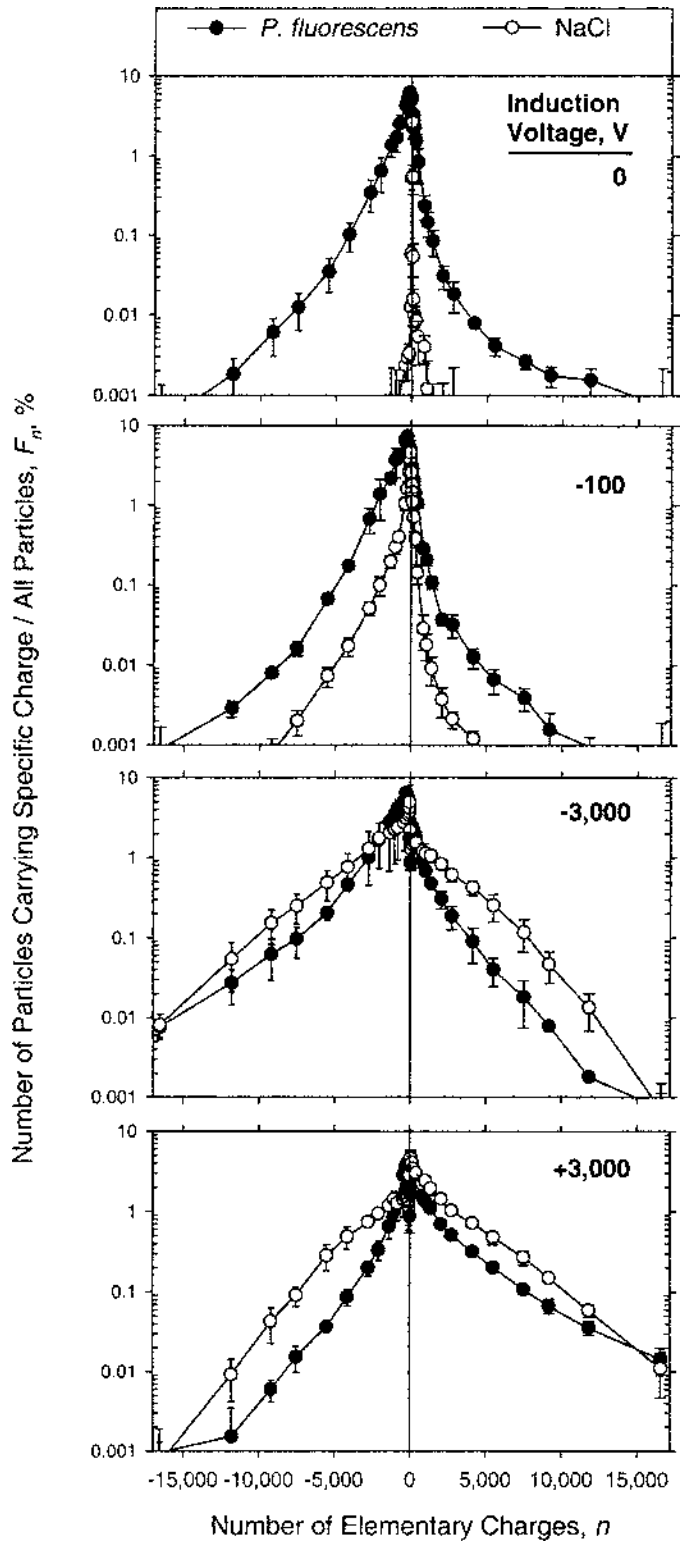


**Figure 7.** Charge distributions of *P. fluorescens* bacteria (0.65–0.8 $\mu$m) and NaCl particles (0.65–0.8 $\mu$m) at different charging conditions, shown over wide elementary charge range.

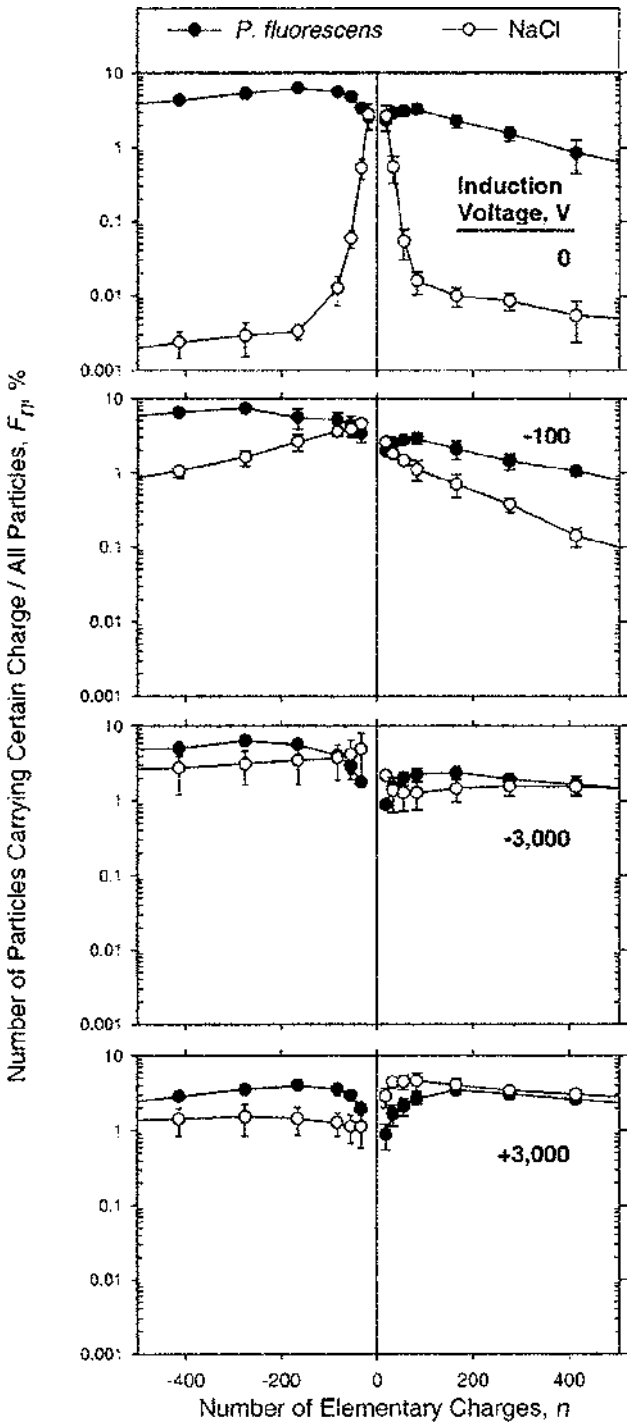


**Figure 8.** Charge distributions of *P. fluorescens* bacteria (0.65–0.8 $\mu$m) and NaCl particles (0.65–0.8 $\mu$m) at different charging conditions, shown near the 0 charge level.

on them by the dispersion process. However, at this time the exact contribution of each component is unclear. This question could be answered by future research. In contrast, the NaCl particles carry only dispersion-imposed charges.

Figures 7 and 8 illustrate that *P. fluorescens* bacteria and NaCl particles respond to external charging very differently. This difference can be explained by the different nature of these particles, as discussed above. According to Reischl et al. (1977), conductive solutions accept induction charging very well, while poor conductors do not. They also observed that the charge on residual particles from distilled water droplets (very poor conductor) are the same, irrespective of the level of induction voltage. In our case, the conductivities of NaCl and *P. fluorescens* solutions were 1,650 $\mu$S and 0 $\mu$S, respectively, as measured with a conductivity meter (Oakton TDSTestr 3, Cole-Parmer Instrument Company, Vernon Hills, IL). Although the bacterial suspension is a very poor conductor, application of a high induction voltage increased the number of highly charged bacteria more than 10 times, as seen in the left-hand charts of Figure 5. This shows that the bacterial particles may be conductive due to the presence of electric charges in their cell walls. The charges in the cell wall matrix originate from acidic groups such as carboxyl, phosphate, and amino groups, which may be present in high concentrations (Van der Wal et al. 1997). However, the fact that the bacteria do not accept external charging as readily as the NaCl particles indicates that bacteria may have their own mechanisms for regulating their electric charges.

## CONCLUSIONS

The experiments with *P. fluorescens* bacteria and NaCl particles have shown that the newly built bioaerosol generator with charge induction is capable of aerosolizing and simultaneously charging biological and nonbiological particles. It was also concluded that the experimental setup, in which airborne particles carrying a specific number of electric charges are extracted by our new electric mobility classifier and then analyzed by an optical particle size spectrometer and a bioaerosol sampler, could be used to analyze the electric charges on other biological and nonbiological particles. Our research has shown that aerosolized *P. fluorescens* bacteria have a very wide bipolar charge distribution, which is net negative and can carry up to 13,000 elementary charges per single bacterium. In contrast, nonbiological NaCl particles were found to carry very few electric charges when they are aerosolized in the same manner from a conductive solution with no induction voltage applied. We have concluded that the electric charge carried by a bacterium consists of 2 components: its own natural charge, which can be high, and the charge imposed on it by the dispersion process. However, at this time the exact contribution of each component is unclear. If the natural charge component on airborne microorganisms is sufficiently high, their collection by electrical field forces may be possible even without charging them. Measurements of microorganism charge in residential and occupational environments may provide an answer to that question.

## REFERENCES

Atten, A., and Oliveri, S. (1992). Charging of Drops Formed by Circular Jet Breakup, *J. Electrostatics* 29:73–91.

Bassett, J. D. (1975). Study of the Charging Mechanisms During the Production of Water Aerosols, *J. Electrostatics* 1:47–60.

Boelter, K. J., and Davidson, J. H. (1997). Ozone Generation by Indoor, Electrostatic Air Cleaners, *Aerosol Sci. Technol*. 27:689–708.

Brown, R. C. (1997). Tutorial Review: Simultaneous Measurement of Particle Size and Particle Charge, *J. Aerosol Sci*. 28:1373–1391.

Chen, S.-K., Vesley, D., Brosseau, L. M., and Vincent, J. H. (1994). Evaluation of Single-Use Masks and Respirators for Protection of Health Care Workers against Mycobacterial Aerosols, *Amer. J. Inf. Control* 22:65–74.

Choi, K.-J., and Delcorio, B. (1990). Generation of Controllable Monodispersed Sprays Using Impulse Jet and Charging Techniques, *Rev. Sci. Instrum*. 61:1689–1693.

Cox, C. S., and Wathes, C. M., eds. (1995). *Bioaerosols Handbook*, CRC, Lewis Publishers, Boca Raton, FL.

Erin, T., and Hendricks, C. D. (1968). Uniform Charged Solid Particle Production, *Rev. Sci. Instrum*. 39:1269–1271.

Forsyth, B., Liu, B. Y. H., and Romay, F. J. (1998). Particle Charge Distribution Measurement for Commonly Generated Laboratory Aerosols, *Aerosol Sci. Technol.* 28:489–501.

Gorny, R. L., and Dutkiewicz, J. (1998). Evaluation of Microorganisms and Endotoxin Levels of Indoor Air in Living Rooms Occupied by Cigarette Smokers and Non-smokers in Sosnowiec, Upper Silesia, Poland, *Aerobiologia* 14:235–239.

Heikkinen, M. S. A. (2000). Experimental Investigation of Sintered Porous Metal Filters, *J. Aerosol Sci.* 31:721–738.

Hendricks, C. D. (1973). Charging Microscopic Particles. In *Electrostatics and its Applications*, edited by E. Moore. John Wiley & Sons, New York, pp. 57–85.

Hirabayashi, A., and de la Mora, F. J. (1998). Charged Droplet Formation in Sonic Spray, *Intern. J. Spectrom. Ion Proces*. 175:277–282.

Huang, S.-L., Ting, L.-W., and Shian-Jang, S. (1996). The Comparative Performance Test of Respirator Cartridges, *J. Aerosol Sci*. 27:655.

Jensen, P. A., Todd, W. F., Davis, G. N., and Scarpino, P. V. (1992). Evaluation of Eight Bioaerosol Samplers Challenged with Aerosols of Free Bacteria, *Am. Ind. Hyg. Assoc. J.* 53:660–667.

Jensen, P. A., Lighthart, B., Mohr, A. J., and Schaffer, B. T. (1994). Instrumentation Used with Microbial Bioaerosol. In *Atmospheric Microbial Aerosols, Theory and Applications*, edited by B. Lighthart and A. J. Mohr. Chapman and Hall, New York, pp. 226–284.

Johnston, A. M., Vincent, J. H., and Jones, A. D. (1985). Measurements of Electric Charge for Workplace Aerosols, *Appl. Occup. Hyg.* 29:271–284.

Mainelis, G., Grinshpun, S. A., Willeke, K., Reponen, T., Ulevicius, V., and Hintz, P. J. (1999). Collection of Airborne Microorganisms by Electrostatic Precipitation, *Aerosol Sci. Technol*. 30:127–144.

May, K. R. (1973). The Collison Nebulizer: Description, Performance and Application, *J. Aerosol Sci.* 4:235–243.

Neidhardt, F. C., Ingraham, J. L., and Schaechter, M. (1990). *Physiology of the Bacterial Cell: A Molecular Approach*, Sinauer Associates, Inc., Sunderland, MA.

Nevalainen, A. (1989). *Bacterial Aerosols in Indoor Air*, National Public Health Institute, Kuopio, Finland.

Palleroni, N. J. (1984). Family I. *Pseudomonadacae*. In *Bergey's Manual of Systematic Bacteriology*, edited by N. R. Kreig and J. G. Holt. The Williams and Wilkins Co., Baltimore, MD, Vol. 1, p. 165.

Periasamy, R., Clayton, A. C., Lawless, P. A., Donovan, R. P., and Ensor, D. S. (1991). Generation of Uniformly Sized, Charged Particles in a Vacuum, *Aerosol Sci. Technol*. 15:256–265.

Qian, Y., Willeke, K., Ulevicius, V., and Grinshpun, S. A. (1997). Particle Reentrainment from Fibrous Filters, *Aerosol Sci. Technol*. 27:394–404.

Qian, Y., Willeke, K., Ulevicius, V., Grinshpun, S. A., and Donnelly, J. (1995). Dynamic Size Spectrometry of Airborne Microorganisms: Laboratory Evaluation and Calibration, *Atmos. Environ*. 29:1123–1129.

Reischl, G., John, W., and Devor, W. (1977). Uniform Electrical Charging of Monodisperse Aerosols, *J. Aerosol Sci.* 8:55–65.

Sherbet, G. V., and Lakshmi, M. S. (1973). Characterisation of *Escherichia coli* Cell Surface by Isoelectric Equilibrium Analysis, *Biochim. Biophys. Acta* 298:50–58.

Stewart, S. L., Grinshpun, S. A., Willeke, K., Terzieva, S., Ulevicius, V., and Donnelly, J. (1995). Effect of Impact Stress on Microbial Recovery on an Agar Surface, *Appl. Environ. Microbiol.* 61:1232–1239.

Terzieva, S., Donnelly, J., Ulevicius, V., Grinshpun, S. A., Willeke, K., Stelma, G. N., and Brenner, K. P. (1996). Comparison of Methods for Detection and Enumeration of Airborne Microorganisms Collected by Liquid Impingement, *Appl. Environ. Microbiol.* 62:2264–2272.

Van der Wal, A., Minor, M., Norde, W., Zehnder, A. J. B., and Lyklema, J. (1997). Conductivity and Dielectric Dispersion of Gram-Positive Bacterial Cells, *J. Colloid Interface Sci*. 186:71–79.